ACS APPLIED MATERIALS & INTERFACES

Research Article

www.acsami.org

Colloidal Stability of Silk Fibroin Nanoparticles Coated with Cationic Polymer for Effective Drug Delivery

Suhang Wang,[†] Tao Xu,[†] Yuhong Yang,[‡] and Zhengzhong Shao*[,†]

[†]State Key Laboratory of Molecular Engineering of Polymers, Department of Macromolecular Science and Laboratory of Advanced Materials, and [‡]Research Center for Analysis and Measurement, Fudan University, Shanghai 200433, P.R. China

Supporting Information

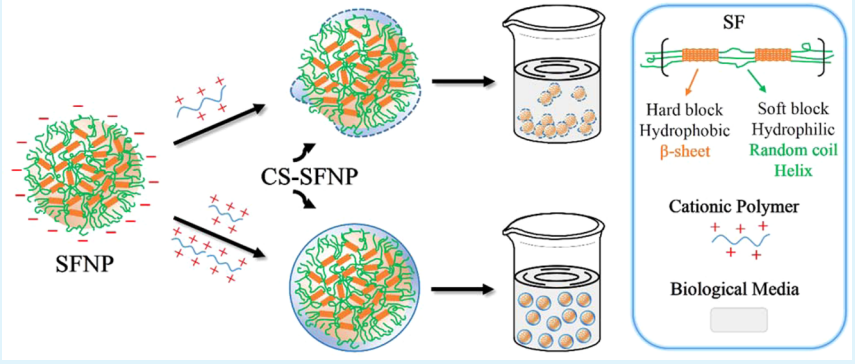

ABSTRACT: Generally, silk fibroin nanoparticles (SFNPs) are great candidates to deliver drugs or other bioactive substances in vivo. However, their further applications are largely limited by the low colloidal stability of SFNPs, as they tend to aggregate in biological media. To address this issue, SFNP composite materials with a core−shell structure (CS-SFNPs) were fabricated by coating SFNPs with four different selected cationic polymers, glycol chitosan, *N*,*N*,*N*-trimethyl chitosan, polyethylenimine, and PEGylated polyethylenimine, through electrostatic interaction. According to the DLS and NTA results, compared with the bare SFNPs, the CS-SFNPs showed much higher colloidal stability in biological media. When treated with human cervical carcinoma (HeLa) cells, the CS-SFNPs were efficiently internalized and accumulated in lysosome; and when loaded with an anticancer drug, DOX, the CS-SFNPs also showed higher cytotoxicity against HeLa cells. Our results suggest that the fabricated CS-SFNPs with desirable colloidal stability in biological media have the potential to be employed as drug carriers for the anticancer drug delivery system.

KEYWORDS: *silk fibroin nanoparticle, cationic polymer, core−shell structure, colloidal stability, biological media*

1. INTRODUCTION

Nanoparticles have attracted increasing attention in recent years since they have shown great potential for a wide variety of applications in many fields, such as electronics, catalytic chemistry, biology, medicine, etc.[1−3] With the rapid development of nanotechnology and nanomedicine, nanosized materials are playing increasingly important roles in the field of biological medicine. However, the more comprehensive application of nanoparticles in biological medicine is still subject to certain difficulties, one of which is the colloidal stability of nanoparticles in biological systems.[4,5] When nanoparticles are transferred into biological media (e.g., Dulbecco's modified Eagle's medium (DMEM) or 0.01 mol/L phosphate buffered saline (PBS)), their intrinsic properties, such as size, surface charges, aggregation state, etc., could significantly change in response to the physicochemical properties of the solution (e.g., ionic strength, pH, temperature and components).[6,7] The ionic strength in biological media is often around 150 mmol/L, meaning that the electrostatic forces are most likely to be screened within a few nanometers of the surface, thereby leading to the formation of aggregation.[8] Most nanoparticles have a tendency to aggregate in biological media,[4,5,7,8] which may result in precipitation. Precipitation would be deleterious and perilous if these particles are injected intravenously. On the other hand, since the minimum diameter of capillaries in the body is 4 μm, microsized particles and/or aggregations of nanoparticles may be trapped, causing emboli in the capillary bed.[5,9] Therefore, agglomeration of nanoparticles in biological media must be avoided.

The current state-of-the-art methods of stabilizing nanoparticles against aggregation in biological media are mainly focused on the modification or functionalization of the surfaces of nanoparticles with natural or synthetic polymers. Natural polymers, such as chitosan, alginate, dextran, etc., have been employed to coat magnetic (Fe_3O_4) nanoparticles and carbon nanotubes; and the fabricated composites have shown colloidal

Received: June 16, 2015
Accepted: September 2, 2015
Published: September 2, 2015

DOI: 10.1021/acsami.5b05335
ACS Appl. Mater. Interfaces 2015, 7, 21254−21262

stability in water for a wide range of pH, as well in commonly used biological buffers.[7,9−11] As for synthetic polymers, hydrophilic poly(ethylene glycol) (PEG) has been regarded as an effective coating materials for nanoparticles because of its ability to resist protein fouling and to provide steric hindrance to prevent the aggregation of nanoparticles.[12,13] Furthermore, PEGylation of nanoparticles shows favorable effect on reducing the reticuloendothelial system clearance and prolonging their lifetime in blood circulation, which contributes to the chance of their accumulation in tumors.[14] Though certain improvements have been made by these studies, developing a reasonably stable polymeric coating that could endow nanoparticles with desirable colloidal stability in biological media still remains challenging.

In the past decades, silk fibroin (SF), a protein derived from the domestic silkworm (*Bombxy mori*) or wild silkworm (*A. pernyi*) silk, has been widely investigated in biomedical and pharmaceutical fields because of its remarkable mechanical properties, good biocompatibility, controllable biodegradability and low immunogenicity.[15−18] Recently, various SF-based biomaterials, including films, scaffolds, hydrogels, fibers, etc.,[19] have been prepared under mild processing and chemical modification free conditions, suggesting that SF is an ideal candidate to be applied in biomedicine. To date, many efforts, such as phase separation,[20] salting out,[21] and spray-drying[22] have been employed to develop silk particles as drug delivery carrier. Particularly, some water-miscible organic solvents can induce the aggregation of SF to produce submicrometer particles,[23−25] which are considered to be beneficial for the cellular and tissue uptake. To the best of our knowledge, though a number of studies have reported the therapeutic promise of SFNPs in vitro,[25−28] few reports have been published on the in vivo experiment of SFNPs for anticancer drug delivery. Physicochemical properties of SFNPs could be significantly changed by the complex microenvironment in vivo before SFNPs being taken by cells. Comprehensive investigation of the colloidal stability, surface charge, and aggregation state of SFNPs as well as their interaction with cells is essential for in-depth understanding of the cellular uptake mechanism.

Regarding the application of SFNPs in biomedicines, a major problem lies in their tendency to aggregate, especially in biological media with high ionic strength. To tackle this problem, this study is designed to develop SFNP composites with desirable colloidal stability in biological media via surface modification. Four different cationic polymers, including natural and synthetic polymers: glycol chitosan (GCS), *N,N,N*-trimethyl chitosan (TMC), polyethylenimine (PEI) and PEGylated polyethylenimine (PEG−PEI), were coated onto the SFNPs through electrostatic interaction, respectively. Colloidal stabilities of these modified SFNPs in water, biological standard buffers (e.g., PBS) and cell culture media (e.g., DMEM) were examined by dynamic light scattering (DLS) and nanoparticle tracking analysis (NTA). Cytotoxicity of two kinds of doxorubicin (DOX)-loaded modified SFNPs was investigated using HeLa cells by the Cell Counting Kit-8 (CCK-8) assay.

2. MATERIALS AND METHODS

2.1. Materials. The cocoons of *Bombyx mori* silkworm were obtained from Jiangsu Province, China. GCS (degree of polymerization ≥400), PEI (branched, M_w = 25 000, M_n = 10 000) and mPEG (M_n = 2000) were purchased from Sigma-Alderich Co. LLC (USA). Methoxy polyethylene glycol amine (mPEG-NH_2), Rhodamine B isothiocyanate (RITC) and Fluorescein isothiocyanate (FITC) were purchased from Aladdin. PBS was purchased from Hangzhou Genom Biotech Co., Ltd. (China). DOX was obtained from Beijing Huafeng United Technology Co., Ltd. (China). CCK-8 was purchased from Dojindo Laboratorise, Japan. Gibco fetal bovine serum (FBS), Gibco DMEM and LysoTracker Probes labeling kit were supplied by Invitrogen (Waltham, MA, USA). The other chemicals were all purchased and used as received without further purification if not specified. All nanoparticle stock solutions were prepared using pure deionized water (resistivity >18 MΩ cm).

2.2. Synthesis of TMC and PEG−PEI. TMC was synthesized and characterized following our established procedures.[29] Details about the synthesis of PEG−PEI are described in the Supporting Information.

2.3. Preparation of Regenerated SF Solution. Degumming of *Bombyx mori* silk and the preparation of regenerated SF solutions were conducted according to the established procedures.[30] Briefly, the silkworm cocoons were cut into small pieces and boiled in 0.5% Na_2CO_3 solution for 60 min, and then rinsed with abundant deionized water to remove the sericin. The resulting degummed silk fiber was dissolved in a ternary system ($CaCl_2$/ethanol/H_2O at 1:2:8 mol ratio) at 90 °C for 2 h. The SF-salts solution was filtered to remove the impurities, and then dialyzed continuously for 3 days against running deionized water using a cellulose semipermeable membrane (molecular weight cutoff (MWCO), 12−14 kDa). The resulting regenerated SF solution was stored at 4 °C.

2.4. Preparation of SFNPs. The preparation of SFNPs was carried out mainly based on the method previously reported[23] with a slight modification. Briefly, the regenerated SF solution with 4.0 wt % of SF was rapidly introduced into at least 90% (v/v) of the final mixture volume of water-miscible acetone using a sample pipet at room temperature. Milk-like SFNPs were formed upon addition, and the resulting SFNP suspension was stirred at room temperature to remove acetone. The as-prepared SFNP suspension was stored at 4 °C.

2.5. Fabrication of Polymer/SFNPs Composites. SFNP suspension was mixed with the cationic polymer solutions (GCS, TMC, PEI, and PEG−PEI), respectively, at different mass ratios. For example, 1 mL GCS (10 μg/mL) solution was added to 1 mL SFNPs (100 μg/mL) suspension, which means the mass ratio of GCS to SFNPs was 0.1. In this paper, the products are referred to as SFNP@GCS, SFNP@TMC, SFNP@PEI, and SFNP@(PEG−PEI), respectively.

2.6. Particle Size and Zeta-Potential Analysis. The particle sizes and zeta-potentials of SFNPs and polymer/SFNP composites were measured at 25 °C with a Zetasizer Nano instrument (Malvern Inst. Ltd., UK) equipped with DLS (He−Ne laser, 633 nm wavelength) and a standard capillary electrophoresis cell, respectively. The concentration of SFNP was 10 μg/mL and the total volume was 1 mL. The Stokes−Einstein relationship and Smoluchowski model were used for the analysis of particle size and zeta-potential, respectively. Transmission electron microscopy (TEM) examination was performed with a FEI Tecnai G^2 instrument at 200 kV. For sample preparation, diluted suspension was dropped on a copper grid and allowed to dry slowly.

2.7. Stability Tests in Water and in Various Biological Media. To test the stability of SFNPs and polymer/SFNP composites in various culture media, we respectively added 200 μL suspension of SFNPs or polymer/SFNP composites (containing 10 μg SFNPs) to 800 μL of water, serum-free DMEM, and PBS (0.01 mol/L pH 7.4), and then incubated it at 37 °C for 24 h. The particle sizes and zeta-potentials of SFNPs and their composites were measured as described above. Data were obtained by measuring three independent sample batches.

2.8. Preparation of DOX-Loaded SFNPs. DOX was dissolved in water and then added to the as-prepared SFNPs (62.5 μg/mg), followed by an adsorption period of 20 h at room temperature under dynamic conditions. The particles were collected by centrifugation at 20 000 × g for 40 min. The amount of drug remaining in the solution was determined by Hitachi UV 2910 UV−vis spectrometer. Drug loading and the efficiency of encapsulation were calculated as follows

DOI: 10.1021/acsami.5b05335
ACS Appl. Mater. Interfaces 2015, 7, 21254−21262

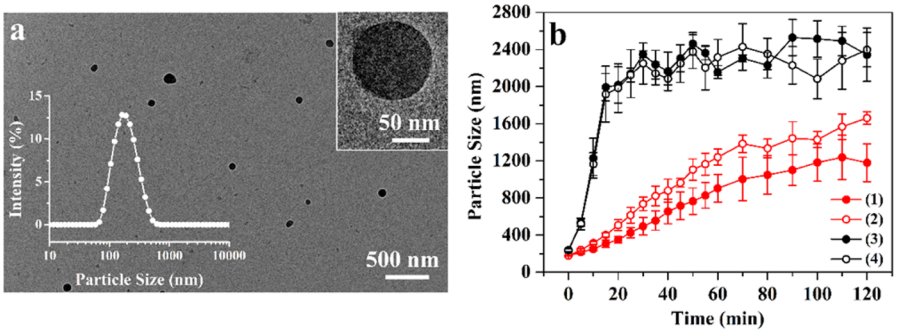

Figure 1. Characterization of SFNPs. (a) TEM images of SFNPs. The insets showed the SFNP in higher magnification and the size distribution of SFNPs measured by DLS. (b) Particle sizes of SFNPs prepared with acetone or ethanol as a function of time in serum-free DMEM or 0.01 mol/L PBS. (1) SFNPs prepared with acetone in serum-free DMEM; (2) SFNPs prepared with acetone in 0.01 mol/L PBS; (3) SFNPs prepared with ethanol in serum-free DMEM; and (4) SFNPs prepared with ethanol in 0.01 mol/L PBS.

$$\text{drug loading (\%)} = \frac{W_D}{W_S} \times 100\%$$

$$\text{encapsulation efficiency (\%)} = \frac{W_D}{W_F} \times 100\%$$

where W_D represents the weight of the DOX in SFNPs, W_S is the weight of the SFNPs, and W_F is the weight of the feeding DOX.

After that, cationic polymers were added in the suspension to produce polymer/SFNP composites that encapsulated DOX. To investigate the redispersion ability of the drug loaded composites in the media, we lyophilized the obtained suspension.

2.9. In Vitro Release of DOX-Loaded Polymer/SFNP Composites. The free DOX, lyophilized (SFNP/DOX)@GCS and (SFNP/DOX)@(PEG−PEI) were dispersed in 0.5 mL PBS (0.01 mol/L, pH 7.4), respectively. The suspension was placed in a dialysis tube (MWCO = 12−14 kDa) and immerged into 1 mL PBS (0.01 mol/L, pH 7.4) at 37 °C in a constant temperature shaker for 6 days. At predetermined time points, the DOX concentration in the released medium was determined by UV absorption; and fresh PBS was added, ensuring that sink conditions were maintained unchanged throughout the experiment.

2.10. Cell Culture. HeLa cells were purchased from the cell bank of Chinese Academy of Science (Shanghai, China). The cells were cultured in DMEM, supplemented with 10% FBS, 100 U/mL penicillin, and 100 μg/mL streptomycin at 37 °C using a humidified 5% CO_2 incubator.

2.11. Colocalization by LSCM. SFNP@GCS was selected to be a representative polymer/SFNP composite for the further analysis of the colocalization of SFNPs with the cationic polymer. Briefly, SFNPs and GCS were labeled by RITC and FITC, respectively.[31] HeLa cells were seeded on a 35 mm glass bottom culture dish at 2×10^5 cells/well with DMEM supplemented with 10% FBS (DMEM-FBS). At ∼ 50% cell confluence, the media were removed and the cells were rinsed twice with serum-free DMEM; and then the cells were replenished with 2 mL DMEM-FBS containing RITC-labeled SFNP and (RITC-labeled SFNP)@(FITC-labeled GCS) (5 μg (RITC-labeled SFNP)/well). After different incubation times, the media were removed and washed several times by PBS, followed by refilling the wells with 2 mL of PBS. Finally, the cells were imaged using laser scanning confocal microscope (LSCM, Olympus Fluoview FV 1000). For colocalization of (RITC-labeled SFNP)@GCS with lysosome, (RITC-labeled SFNP)@GCS was incubated with the cells for 12 h, the media were removed and washed several times by PBS, and then lysotracker was added according to the protocol. Afterward, the cells were imaged using LSCM.

2.12. In Vitro Cytotoxicity Studies. The cytotoxicity of SFNPs and polymer/SFNPs composites with or without DOX against HeLa cells was determined by CCK-8. The cells were seeded in 96-well plates (1×10^4 cells/well) with DMEM-FBS and incubated at 37 °C with 5% CO_2 for 24 h. After removing the medium, 200 μL of DMEM-FBS containing various concentration of SFNP, SFNP@GCS, SFNP@(PEG−PEI), free DOX, SFNP/DOX, (SFNP/DOX)@GCS and (SFNP/DOX)@(PEG−PEI) were added, respectively, and further incubated for different periods of time. Then, the culture medium was replaced with fresh serum-free DMEM; and CCK-8 was added in dark according to the protocol and the absorbance of the solution at 450 nm was tested using an Elx 800 instrument (Biotek, USA) after incubation for 2 h. The relative cell viability (%) was calculated as follows

$$\text{cell viability (\%)} = \frac{[A]_{\text{test}}}{[A]_{\text{control}}} \times 100\%$$

where $[A]_{\text{test}}$ is the absorbance of the test sample and $[A]_{\text{control}}$ is the absorbance of the control sample without material.

2.13. Data Analysis. Differences between the means were investigated using one-way ANOVA analysis and Tukey's test. Differences between the group means were considered significant at $p < 0.05$ (*), $p < 0.01$ (**), and $p < 0.001$ (***); NS, no significant difference, $p > 0.05$.

3. RESULTS AND DISCUSSION

3.1. Characterization of SFNPs. The preparation of SFNPs followed a one-step desolvation procedure. With the rapid introduction of the regenerated SF solution into excessive acetone, the milk-like suspension of SFNPs was formed immediately. As shown in the TEM images in Figure 1a, the SFNPs presented spherical geometry without obvious aggregation. The observed particle sizes of SFNPs were around 100 nm, much smaller than that measured by DLS (168 ± 7 nm). This was mainly due to the dehydration process which led to the shrinkage of the particles in the preparation of TEM samples. The PDI of SFNPs was 0.129 and the zeta-potential was −20.0 ± 5.0 mV.

To the best of our knowledge, a significant challenge in the application of nanoparticles is to retain their stability in the environment of concern. In most cases, SFNPs to be employed in biomedicine will be suspended in biological media, such as DMEM and PBS. In the previous reports, the particle size and aggregation state of SFNPs were only examined in water by DLS.[20,25] However, the properties of the nanoparticles in biological media will change and be different from the initial state.[4] As shown in Figure 1b, the particle sizes of SFNPs prepared with the assistance of different water-miscible organic solvents, such as acetone[23] and ethanol,[24] increased over time as a result of aggregation in serum-free DMEM or in 0.01 mol/L PBS within a few minutes. SF, a biopolymer containing both hydrophobic and hydrophilic blocks, self-assembled in the aqueous solution into a structure with two "phases": the crystalline phase is the well-order "core"; and the amorphous

DOI: 10.1021/acsami.5b05335
ACS Appl. Mater. Interfaces 2015, 7, 21254−21262

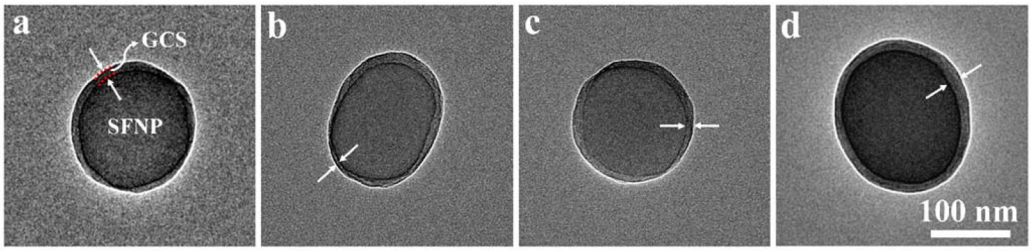

Figure 2. TEM images of SFNPs coated with cationic polymer. (a) SFNP@GCS (the mass ratio of GCS to SFNPs was 0.1); (b) SFNP@TMC (the mass ratio of TMC to SFNPs was 1.5); (c) SFNP@PEI (the mass ratio of PEI to SFNPs was 1); (d) SFNP@(PEG−PEI) (the mass ratio of PEG−PEI to SFNPs was 2). The same scale bar is applied for a−d.

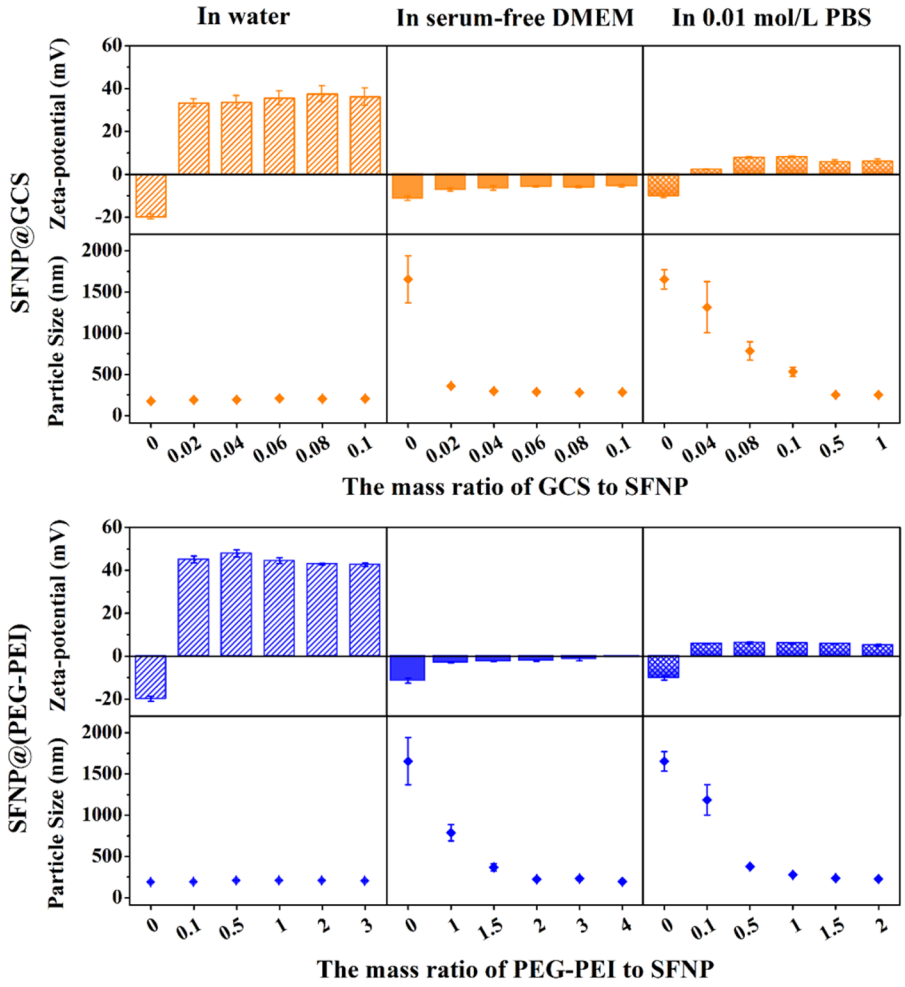

Figure 3. Zeta potentials and particle sizes of SFNPs coated with cationic polymers (GCS or PEG−PEI) at different mass ratios, incubated in water, serum-free DMEM or 0.01 mol/L PBS at 37 °C for 24 h.

phase is the poor-ordered "shell". The intrusion of hydrophilic segments into the solution results in a coarse sphere surface.[24] The loosely packed structures and the coarse sphere surface of SFNPs will be greatly affected by the environment. On the other hand, after the SFNPs are transferred into the biological media, the higher ionic strength of the solution could reduce the electrostatic repulsive forces between the particle surfaces, and consequently lead to aggregation. Therefore, improving the colloidal stability of SFNPs in biological media is a key point for their wider application in the biological field.

3.2. Characterization of Polymer/SFNPs Composites. Given that the surfaces of SFNPs are negatively charged, our design is to modify the surfaces with positively charged natural or synthetic polymers to stabilize SFNPs against aggregation in biological media. Chitosan, a naturally derived polysaccharide, is a promising polycation that has drawn growing attention as drug[32] or gene carrier[33] because of its favorable biocompatibility, biodegradability, and biological activities. However, chitosan manifests acid-solubility and is normally insoluble where the pH of the solution is above 6. Therefore, much effort has been made to modify chitosan to improve its solubility. Among the different chitosan derivatives with improved hydrophilicity, GCS[34] and TMC,[29] have captured much attention as novel carriers for drugs and genes because of the good solubility in a broad range of pH and the favorable biocompatibility. Besides the natural polymers, two synthetic

DOI: 10.1021/acsami.5b05335
ACS Appl. Mater. Interfaces 2015, 7, 21254−21262

polymers, PEI and PEG−PEI, have also been investigated. Cationic PEI is considered to be one of the most efficient candidates to deliver genes and often serves as a "golden standard".[35] PEG−PEI, prepared by the covalent attachment of PEG segments to PEI molecules, has considerably reduced adverse effects on cell viability, compared with PEI; and shows a longer circulation time in vivo because of the reduced nonspecific interactions with serum albumin and cellular components in the bloodstream.[36] In this work, these four different cationic polymers were successfully coated onto the surfaces of SFNPs through electrostatic interaction. It can be seen in Figure 2 that the products (polymer/SFNPs composites) presented a core−shell structure: the cationic polymer shell is coated on the SFNP core. In the following discussion, the polymer/SFNPs composites are referred to as CS-SFNPs. Particle sizes of CS-SFNPs measured by DLS were 180−200 nm; and the zeta potentials were presented from negative to positive (Figure 3 and Figure S1).

3.3. Stability of SFNP and CS-SFNPs in Water and in Various Biological Media. As shown in Figure 3 and Figure S1, the SFNPs were stable and dispersed well in water for a relatively long period of time. In fact, the suspension can be stored at 4 °C for at least 1 month without obvious aggregation. In contrast, agglomeration was observed in biological media. This is probably because the attraction force between the SFNPs becomes higher than the repulsive force as the ionic strength of the media increases. By comparison, no evident increase of the particle sizes of the CS-SFNPs was observed under the same conditions, indicating the significantly enhanced stability of the CS-SFNPs in biological media. In serum-free DMEM, SFNP@GCS, SFNP@TMC, SFNP@PEI, and SFNP@(PEG−PEI) became stable when the critical ratios of polycations to SFNP reached 0.06, 1.5, 1, and 2, respectively. In 0.01 mol/L PBS, those critical ratios were 0.5, 1.5, 1, and 2, respectively. In this paper, the critical ratio refers to the minimum mass ratio required to keep the particles stable (against aggregation) in media. If the SFNPs are coated with TMC at a ratio below the critical ratios (e.g., 0.1 and 0.5), the SFNPs cannot be sufficiently covered, shown in Figure S2. The incomplete coating is not able to prevent the aggregation of the nanoparticles in the biological environment. When the amount of TMC increases to the critical ratio of 1.5, the SFNPs are covered by a relatively perfect shell of a tightly bound polymer layer; and a stable dispersal system is formed (Figure 2b and Figure 3). It should be noted that not all polycations present the same result. In a previous report, Yu et al.[26] improved the uniformity of the redispersed silk nanospheres in water by adding mPEG-NH_2. However, even when the mass ratio of mPEG-NH_2 to SFNP reached 4, the particle size and zeta-potential of SFNP@(mPEG-NH_2) (i.e., 178 ± 5 nm and −22.0 ± 1.1 mV) were still close to those of the SFNPs; and the modified nanoparticles were still unstable in biological media (Figure S3). This may resulted from the lack of positive charges (which play an essential role in the formation of a core−shell structure via electrostatic interaction) in the polymer chain: only one amino group and long PEG tail (considering the steric hindrance) in one PEG molecular chain.

Biological media are commonly used to mimic the pH, osmomolarity, and saline conditions in blood. Nevertheless, there are proteins and other biomolecules present in blood; and therefore, performance of the nanoparticles in blood is not always the same as that in serum-free biological media. Accordingly, the colloidal stability of the nanoparticles in the presence of serum-supplemented growth media should be investigated. As in known, the major component of FBS is the globular protein bovine serum albumin (BSA). Particle size of BSA is normally several tens of nanometers. In this study, colloidal stabilities of SFNPs and CS-SFNPs systems were examined by DLS; and results were shown and interpreted in the form of hydrodynamic diameters. In DMEM with 10% FBS and no nanoparticles, DLS results showed a Z-average hydrodynamic diameter of 36.5 nm. Meanwhile, several other peaks were observed, which may be attributed to different-sized agglomerates of BSA. Similar results were found in previous reports.[37,38] It was worth noting that there was a major peak at 184 nm (Figure S4), similar size to those of the SFNPs and CS-SFNPs (Figure 1a). Therefore, it is difficult to discriminate the data of the samples from the media background. In other words, hydrodynamic diameters of the particles in DMEM-FBS determined by the use of DLS are not perfectly reliable.

NTA, first commercialized in 2006, is a powerful characterization technique complementary to DLS; and is particularly useful for analyzing nanosized particles or particle aggregates in polydisperse suspensions.[39] More importantly, this technique enables the visualization and recording of nanoparticles in liquids. According to the results of NTA (Figure S5), when incubated in DMEM-FBS, the SFNPs tended to aggregate and form large clusters; and the SFNPs with a size <1 μm only accounts for a small proportion. By contrast, when the SFNPs were coated with GCS or PEG−PEI, more desirable particle dispersion was observed as the mass ratio of GCS or PEG−PEI to SFNP increased. This phenomenon was more evident when the ratio was higher than the critical ratio, at which the CS-SFNPs nearly displayed monodisperse and almost all the particles were about 200 nm. Based on the NTA and the DLS results, the CS-SFNPs showed superior colloidal stability, compared with the SFNPs, both in serum-free and serum-containing DMEM, which could be attributed to the ability of the cationic polymers (i.e., GCS and PEG−PEI) to resist protein fouling.[40,13,14]

In water, the zeta potentials of CS-SFNPs changed from negative to positive upon coating (Figure 3 and Figure S1). In contrast, in biological media, the zeta potentials of CS-SFNPs were remarkably reduced due to the interactions between the particles and the negatively charged components.[29] For example, when the SFNP@(PEG−PEI)s with different mass ratios were incubated in 0.01 mol/L PBS, the surface charges were determined to be 5 to 6.2 mV. When they were incubated in serum-free DMEM, the particles exhibited negative charges between −2.9 to −0.5 mV. It can be seen that the media have a significant impact on particle net charge, which remains to be an issue to be addressed.[41] Moreover, the absolute value of the zeta-potentials of SFNP@(PEG−PEI) both in 0.01 mol/L PBS and in serum-free DMEM were lower than those of the bare SFNPs under the same conditions (−10.2 ± 0.9 and −11.4 ± 1.1 mV, respectively). This could be ascribed to the shielding effect of the PEG chains on the surface charge of the SFNP@(PEG−PEI). Recently, with an effort to stabilize the nanoparticles in the biological environment, PEGylation has been generally applied to introduce hydrophilic noncharge layers to the particle surface. In this way, particle aggregation and nonspecific interactions in the biological environment could be reduced under the influences of steric hindrance and shielding effect.[13,14,42] In this study, a similar result can be interestingly found in the case of SFNP@GCS. As one of the chitosan derivatives, GCS is emerging as a novel drug carrier

DOI: 10.1021/acsami.5b05335
ACS Appl. Mater. Interfaces 2015, 7, 21254−21262

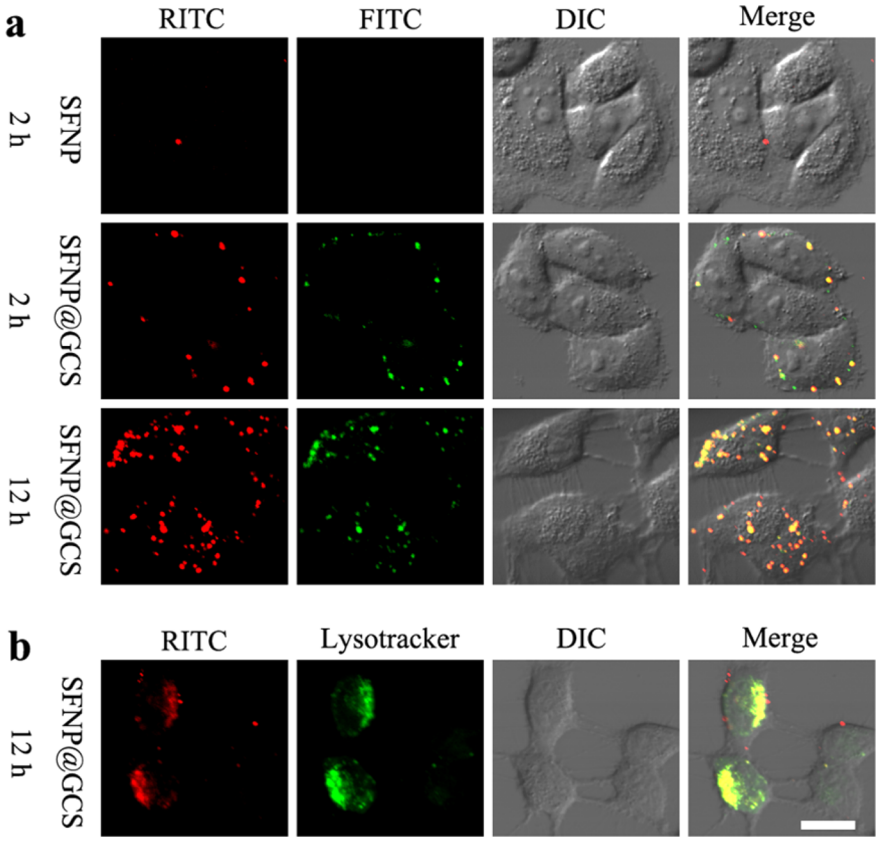

Figure 4. (a) LSCM images of SFNP and SFNP@GCS in HeLa cells at 37 °C under an atmosphere of 5% CO_2. The cells were imaged at 2 or 12 h postincubation. Red, RITC-labeled SFNP; and green, FITC-labeled GCS. (b) LSCM images of SFNP@GCS in HeLa cells imaged at 12 h postincubation. Red, RITC-labeled SFNP; and green, lysotracker-labeled lysosome. Scale bar, 20 μm, applied for both a and b.

Table 1. Particle Sizes and Zeta Potentials of SFNPs, DOX-Loaded SFNPs, SFNP@GCS, and SFNP@(PEG−PEI)

	SFNP	SFNP/DOX	(SFNP/DOX) @GCS	(SFNP/DOX) @(PEG−PEI)
size (nm)	168 ± 7	178 ± 10	201 ± 10	196 ± 4
PDI	0.129	0.192	0.267	0.224
zeta-potential (mV)	−20.0 ± 5.0	−13.2 ± 3.1	5.0 ± 2.6	14.7 ± 2.9

because of its biocompatibility and water solubility.[34] In a previous report,[40] GCS based nanoparticles also displayed long-term circulation in the blood-stream and considerable accumulation in tumor cells. Since GCS and PEG showed similar functions in this context, it is indicated that the $-CH_2-CH_2-O-$ groups, which both GCS and PEG have in common, are most likely to play the role of "shields". On the basis of the results discussed above, we can conclude that it is the steric repulsion of the polymer chains that significantly contribute to the stability of CS-SFNPs in biological media, rather than the electrostatic repulsion between the nanoparticles.

3.4. Cellular Uptake of SFNPs and CS-SFNPs. To further investigate the interactions between SFNP and cationic polymers and the cell trafficking of SFNP and CS-SFNPs, SFNP@GCS with a mass ratio of 0.1, which was stable in DMEM, was selected to be a representative CS-SFNP composite for further analysis. The HeLa cells with different periods of postincubation time were imaged using LSCM. SFNP and GCS were labeled by RITC and FITC, respectively. Figure 4a showed that most of the RITC-labeled SFNPs were colocalized with the FITC-labeled GCS, and could be internalized by and accumulated in the cells. This result confirmed that the cationic polymer was successfully coated onto the SFNPs. However, with the same period of incubation time, much more (RITC-labeled SFNP)@(FITC-labeled GCS) were internalized by the HeLa cells than the RITC-labeled SFNPs. As discussed above, SFNP@GCS demonstrated superior stability in DMEM. On the other hand, the weaker negative charge of SFNP@GCS (−5.6 ± 0.6 mV), compared with that of the SFNP (−11.4 ± 1.1 mV) in serum-free DMEM (Figure 3), may result in weakened electrostatic repulsion forces between the nanoparticles and the cell membranes.[43] Further colocalization between the (RITC-labeled SFNP)@GCS and lysosome showed that most of these nanoparticles accumulated in this organelle (Figure 4b), indicating SFNP@GCS could be trapped in lysosome. On the basis of these results, the CS-SFNPs may be more favorable for further application. Although the differences in cellular uptake efficiency remain to be fully elucidated, to the best of our knowledge, it probably involves nanoparticle stability in cell culture media (i.e., the actual size and surface charge of the internalized nanoparticles including aggregates).

3.5. In Vitro Release of DOX-Loaded SFNP@GCS and SFNP@(PEG−PEI). DOX is one of the most commonly used chemotherapeutic drugs, which interacts with DNA by the intercalation and inhibition of macromolecular biosynthesis.[44]

DOI: 10.1021/acsami.5b05335
ACS Appl. Mater. Interfaces 2015, 7, 21254−21262

In our study, after loading DOX into the SFNPs, the drug loading and encapsulation efficiency were determined to be 5.9 ± 0.1% and 93.6 ± 0.6%, respectively. As listed in Table 1, the particle size of SFNP/DOX was slightly larger than that of SFNP. The aggregation of the bare SFNPs and SFNP/DOX significantly limits their practical applications in the biological environment. Fortunately, the drug-loaded particles still presented negative charges; and therefore can be coated with cationic GCS or PEG−PEI through electrostatic interaction.

In Figure 5, the inset picture shows the redispersion of SFNP/DOX, (SFNP/DOX)@GCS (at the critical ratio of 0.5) and (SFNP/DOX)@(PEG−PEI) (at the critical ratio of 2) in 0.01 mol/L PBS after lyophilization. Unlike SFNP/DOX, which tended to aggregate and precipitate, (SFNP/DOX)@GCS and (SFNP/DOX)@(PEG−PEI) showed desirable redispersibility after lyophilization. Besides, no pronounced changes were observed in the particle sizes and zeta potentials of these samples.

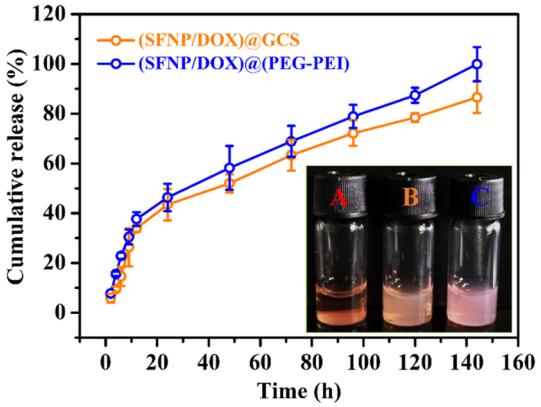

Figure 5. In vitro drug-release curves of DOX-loaded SFNP@GCS and SFNP@(PEG−PEI). The picture inserted showed the redispersion of (A) SFNP/DOX, (B) (SFNP/DOX)@GCS, and (C) (SFNP/DOX)@(PEG−PEI) in 0.01 mol/L PBS after lyophilization.

The potential of these CS-SFNPs to be used as drug carriers was further investigated. As a control, free DOX showed a large burst release (Figure S6), and 79.9 ± 0.3% of DOX was released in the first 12 h. By contrast, only about 30% of DOX loaded in CS-SFNPs was released within the same period of time (Figure 5). The results suggested that DOX release profiles were subject to the release from CS-SFNPs instead of diffusion kinetics through the dialysis tube. A more steady release rate was monitored in a release period of 6 days. It was interesting to find that DOX-release curves of (SFNP/DOX)@GCS and (SFNP/DOX)@(PEG−PEI) were quite similar throughout the whole release period. Besides, both followed a zero-order release after the first day. On the basis of these results, the CS-SFNPs have the potential to be used as drug carriers.

3.6. In Vitro Cytotoxicity Studies. The in vitro cytotoxicity of both free DOX and DOX-loaded particles (SFNP, SFNP@GCS and SFNP@(PEG−PEI)) against HeLa cells were determined by the CCK-8 assay. As shown in Figure 6a1, compared with SFNP/DOX, free DOX and the two kinds of DOX-loaded CS-SFNPs exhibited higher cytotoxicity to HeLa cells at the same dose of DOX (4 μg/mL) after incubated for 6 and 12 h. As a small molecular, free DOX can be quickly transported into cells and enter the active site (nuclei) by passive diffusion. On the other hand, compared with SFNP/DOX, more (SFNP/DOX)@GCS or (SFNP/DOX)@(PEG−PEI) can be internalized in cells. Higher cytotoxicity of (SFNP/DOX)@(PEG−PEI) can be identified in Figure 6a1 than those of the other samples when the incubation time increased to 18 h. Meanwhile, blank samples, SFNP, SFNP@GCS and SFNP@(PEG−PEI) without DOX, showed considerably low cytotoxicity which remained fairly constant with the increase of incubation time, as shown in Figure 6a2. This indicates that the cytotoxicity of the drug-loaded particles mainly resulted from the DOX component rather than the carriers. A similar trend was also observed when the concentration of DOX decreased to 1 μg/mL (Figure 6b1 and b2). Based on the discussion in the previous sections, it was the enhanced colloidal stability of the CS-SFNPs that contributed to the higher cytotoxicity, which makes the CS-SFNPs promising carriers for the anticancer drug delivery system.

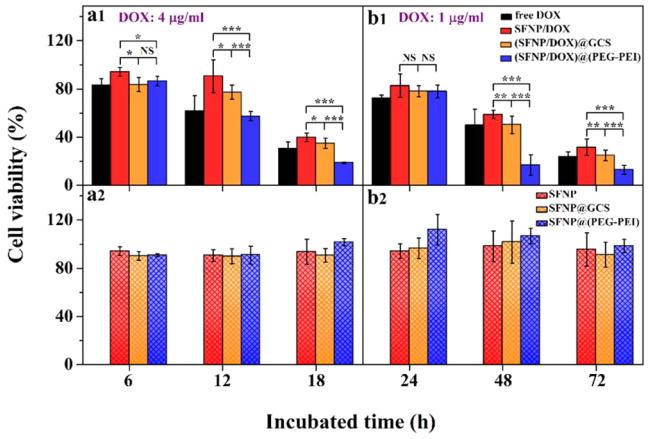

Figure 6. In vitro cytotoxicity studies of SFNP, SFNP@GCS, and SFNP@(PEG−PEI) (a1, b1) with and (a2, b2) without DOX. Cell viabilities of free DOX, SFNP/DOX, (SFNP/DOX)@GCS, and (SFNP/DOX)@(PEG−PEI) at different DOX concentrations (a1, 4 μg/mL; b1, 1 μg/mL) and their blanks (a2 and b2) were examined as a function of incubation time via CCK-8 assay. The *X* axis is the same for a1 and a2, and the *X* axis of b1 and b2 is the same.

4. CONCLUSIONS

In this study, we fabricated the polymer/SFNP composites with a core−shell structure by coating the SFNPs with four different cationic polymers, GCS, TMC, PEI and PEG−PEI. The polymeric coatings significantly enhanced the colloidal stability of SFNPs in biological media. Such enhancement is most likely to result from the steric repulsion of the polymer chains in the shell. Furthermore, DOX-loaded SFNP@GCS and SFNP@(PEG−PEI) showed better redispersibility after lyophilization, which makes possible the wider practical applications of these composite materials. According to the in vitro cell studies, compared with the DOX-loaded SFNP, DOX-loaded SFNP@GCS and SFNP@(PEG−PEI) showed higher cytotoxicity against HeLa cells. Based on our results, CS-SFNPs with desirable colloidal stability in biological media could potentially be more widely applied in vivo; and particularly, they are promising carriers for the anticancer drug delivery system.

■ ASSOCIATED CONTENT

Supporting Information

The Supporting Information is available free of charge on the ACS Publications website at DOI: 10.1021/acsami.5b05335.

DOI: 10.1021/acsami.5b05335
ACS Appl. Mater. Interfaces 2015, 7, 21254−21262

Synthesis of PEG−PEI; nanoparticle tracking analysis; stability test of SFNP@TMC and SFNP@PEI in water and in various biological media; TEM images of SFNP@TMC with the mass ratios of 0.1 and 0.5; stability test of SFNP@(mPEG-NH_2) in various biological media; size distribution of DMEM-FBS measured by DLS; colloidal stability of SFNP, SFNP@GCS, and SFNP@(PEG−PEI) in DMEM-FBS measured by NTA. In vitro drug release curve of free DOX (PDF)

AUTHOR INFORMATION

Corresponding Author

*E-mail: zzshao@fudan.edu.cn.

Notes

The authors declare no competing financial interest.

ACKNOWLEDGMENTS

This work was supported by National Natural Science Foundation of China (No. 21034003, 21374020). We thank Prof. Xin Chen, Dr. Jinrong Yao, Xia Zhang, and Han Cao at Fudan University and Dr. Jie Mei in Malvern Inst. Ltd. for their valuable discussions, and Yiming Zhong (Curtin University, Australia) for critical reading and polishing the English.

REFERENCES

(1) Talapin, D. V.; Lee, J. S.; Kovalenko, M. V.; Shevchenko, E. V. Prospects of Colloidal Nanocrystals for Electronic and Optoelectronic Applications. *Chem. Rev.* **2010**, *110*, 389−458.

(2) Brigger, I.; Dubernet, C.; Couvreur, P. Nanoparticles in Cancer Therapy and Diagnosis. *Adv. Drug Delivery Rev.* **2012**, *64*, 24−36.

(3) Xie, J.; Lee, S.; Chen, X. Y. Nanoparticle-Based Theranostic Agents. *Adv. Drug Delivery Rev.* **2010**, *62*, 1064−1079.

(4) Graf, C.; Gao, Q.; Schutz, I.; Noufele, C. N.; Ruan, W. T.; Posselt, U.; Korotianskiy, E.; Nordmeyer, D.; Rancan, F.; Hadam, S.; Vogt, A.; Lademann, J.; Haucke, V.; Ruhl, E. Surface Functionalization of Silica Nanoparticles Supports Colloidal Stability in Physiological Media and Facilitates Internalization in Cells. *Langmuir* **2012**, *28*, 7598−7613.

(5) Fang, C.; Bhattarai, N.; Sun, C.; Zhang, M. Q. Functionalized Nanoparticles with Long-Term Stability in Biological Media. *Small* **2009**, *5*, 1637−1641.

(6) Stark, W. J. Nanoparticles in Biological Systems. *Angew. Chem., Int. Ed.* **2011**, *50*, 1242−1258.

(7) Saleh, N. B.; Pfefferle, L. D.; Elimelech, M. Influence of Biomacromolecules and Humic Acid on the Aggregation Kinetics of Single-Walled Carbon Nanotubes. *Environ. Sci. Technol.* **2010**, *44*, 2412−2418.

(8) Ji, Z. X.; Jin, X.; George, S.; Xia, T. A.; Meng, H. A.; Wang, X.; Suarez, E.; Zhang, H. Y.; Hoek, E. M. V.; Godwin, H.; Nel, A. E.; Zink, J. I. Dispersion and Stability Optimization of TiO_2 Nanoparticles in Cell Culture Media. *Environ. Sci. Technol.* **2010**, *44*, 7309−7314.

(9) Neuberger, T.; Schopf, B.; Hofmann, H.; Hofmann, M.; von Rechenberg, B. Superparamagnetic Nanoparticles for Biomedical Applications: Possibilities and Limitations of a New Drug Delivery System. *J. Magn. Magn. Mater.* **2005**, *293*, 483−496.

(10) Lopez-Cruz, A.; Barrera, C.; Calero-DdelC, V. L.; Rinaldi, C. Water Dispersible Iron Oxide Nanoparticles Coated with Covalently Linked Chitosan. *J. Mater. Chem.* **2009**, *19*, 6870−6876.

(11) Xu, X. Q.; Shen, H.; Xu, J. R.; Xie, M. Q.; Li, X. J. The Colloidal Stability and Core-Shell Structure of Magnetite Nanoparticles Coated with Alginate. *Appl. Surf. Sci.* **2006**, *253*, 2158−2164.

(12) Kaaki, K.; Herve-Aubert, K.; Chiper, M.; Shkilnyy, A.; Souce, M.; Benoit, R.; Paillard, A.; Dubois, P.; Saboungi, M. L.; Chourpa, I. Magnetic Nanocarriers of Doxorubicin Coated with Poly(ethylene glycol) and Folic Acid: Relation between Coating Structure, Surface Properties, Colloidal Stability, and Cancer Cell Targeting. *Langmuir* **2012**, *28*, 1496−1505.

(13) Cauda, V.; Argyo, C.; Bein, T. Impact of Different PEGylation Patterns on the Long-Term Bio-Stability of Colloidal Mesoporous Silica Nanoparticles. *J. Mater. Chem.* **2010**, *20*, 8693−8699.

(14) Liu, X. S.; Huang, N.; Wang, H. B.; Li, H.; Jin, Q.; Ji, J. The Effect of Ligand Composition on the in Vivo Fate of Multidentate Poly(Ethylene Glycol) Modified Gold Nanoparticles. *Biomaterials* **2013**, *34*, 8370−8381.

(15) Shao, Z. Z.; Vollrath, F. Surprising Strength of Silkworm Silk. *Nature* **2002**, *418*, 741.

(16) Borkner, C. B.; Elsner, M. B.; Scheibel, T. Coatings and Films Made of Silk Proteins. *ACS Appl. Mater. Interfaces* **2014**, *6*, 15611−15625.

(17) Omenetto, F. G.; Kaplan, D. L. New Opportunities for an Ancient Material. *Science* **2010**, *329*, 528−531.

(18) Hogerheyde, T. A.; Suzuki, S.; Stephenson, S. A.; Richardson, N. A.; Chirila, T. V.; Harkin, D. G.; Bray, L. J. Assessment of Freestanding Membranes Prepared from Antheraea Pernyi Silk Fibroin as a Potential Vehicle for Corneal Epithelial Cell Transplantation. *Biomed. Mater.* **2014**, *9*, 025016.

(19) Rockwood, D. N.; Preda, R. C.; Yucel, T.; Wang, X. Q.; Lovett, M. L.; Kaplan, D. L. Materials Fabrication from Bombyx Mori Silk Fibroin. *Nat. Protoc.* **2011**, *6*, 1612−1631.

(20) Wang, X. Q.; Yucel, T.; Lu, Q.; Hu, X.; Kaplan, D. L. Silk Nanospheres and Microspheres from Silk/PVA Blend Films for Drug Delivery. *Biomaterials* **2010**, *31*, 1025−1035.

(21) Lammel, A. S.; Hu, X.; Park, S. H.; Kaplan, D. L.; Scheibel, T. R. Controlling Silk Fibroin Particle Features for Drug Delivery. *Biomaterials* **2010**, *31*, 4583−4591.

(22) Hino, T.; Shimabayashi, S.; Nakai, A. Silk Microspheres Prepared by Spray-drying of an Aqueous System. *Pharm. Pharmacol. Commun.* **2000**, *6*, 335−339.

(23) Zhang, Y. Q.; Shen, W. D.; Xiang, R. L.; Zhuge, L. J.; Gao, W. J.; Wang, W. B. Formation of Silk Fibroin Nanoparticles in Water-Miscible Organic Solvent and Their Characterization. *J. Nanopart. Res.* **2007**, *9*, 885−900.

(24) Cao, Z. B.; Chen, X.; Yao, J. R.; Huang, L.; Shao, Z. Z. The Preparation of Regenerated Silk Fibroin Microspheres. *Soft Matter* **2007**, *3*, 910−915.

(25) Kundu, J.; Chung, Y. I.; Kim, Y. H.; Tae, G.; Kundu, S. C. Silk Fibroin Nanoparticles for Cellular Uptake and Control Release. *Int. J. Pharm.* **2010**, *388*, 242−250.

(26) Yu, S. Y.; Yang, W. H.; Chen, S.; Chen, M. J.; Liu, Y. Z.; Shao, Z. Z.; Chen, X. Floxuridine-Loaded Silk Fibroin Nanospheres. *RSC Adv.* **2014**, *4*, 18171−18177.

(27) Seib, F. P.; Jones, G. T.; Rnjak-Kovacina, J.; Lin, Y. N.; Kaplan, D. L. pH-Dependent Anticancer Drug Release from Silk Nanoparticles. *Adv. Healthcare Mater.* **2013**, *2*, 1606−1611.

(28) Wu, P. Y.; Liu, Q.; Li, R. T.; Wang, J.; Zhen, X.; Yue, G. F.; Wang, H. Y.; Cui, F. B.; Wu, F. L.; Yang, M.; Qian, X. P.; Yu, L. X.; Jiang, X. Q.; Liu, B. R. Facile Preparation of Paclitaxel Loaded Silk Fibroin Nanoparticles for Enhanced Antitumor Efficacy by Locoregional Drug Delivery. *ACS Appl. Mater. Interfaces* **2013**, *5*, 12638−12645.

(29) Xu, T.; Wang, S. H.; Shao, Z. Z. Insight into Polycation Chain Length Affecting Transfection Efficiency by O-Methyl-Free N,N,N-Trimethyl Chitosans as Gene Carriers. *Pharm. Res.* **2014**, *31*, 895−907.

(30) Wang, Q.; Chen, Q.; Yang, Y. H.; Shao, Z. Z. Effect of Various Dissolution Systems on the Molecular Weight of Regenerated Silk Fibroin. *Biomacromolecules* **2013**, *14*, 285−289.

(31) Gong, Z. G.; Yang, Y. H.; Ren, Q. G.; Chen, X.; Shao, Z. Z. Injectable Thixotropic Hydrogel Comprising Regenerated Silk Fibroin and Hydroxypropylcellulose. *Soft Matter* **2012**, *8*, 2875−2883.

(32) Sanyakamdhorn, S.; Agudelo, D.; Tajmir-Riahi, H. A. Encapsulation of Antitumor Drug Doxorubicin and Its Analogue by Chitosan Nanoparticles. *Biomacromolecules* **2013**, *14*, 557−563.

(33) Mao, S. R.; Sun, W.; Kissel, T. Chitosan-Based Formulations for Delivery of DNA and siRNA. *Adv. Drug Delivery Rev.* **2010**, *62*, 12−27.

DOI: 10.1021/acsami.5b05335
ACS Appl. Mater. Interfaces 2015, 7, 21254−21262

(34) Koo, H.; Min, K. H.; Lee, S. C.; Park, J. H.; Park, K.; Jeong, S. Y.; Choi, K.; Kwon, I. C.; Kim, K. Enhanced Drug-Loading and Therapeutic Efficacy of Hydrotropic Oligomer-Conjugated Glycol Chitosan Nanoparticles for Tumor-Targeted Paclitaxel Delivery. *J. Controlled Release* **2013**, *172*, 823−831.
(35) Yue, Y. A.; Jin, F.; Deng, R.; Cai, J. G.; Chen, Y. C.; Lin, M. C. M.; Kung, H. F.; Wu, C. Revisit Complexation Between DNA and Polyethylenimine - Effect of Uncomplexed Chains Free in the Solution Mixture on Gene Transfection. *J. Controlled Release* **2011**, *155*, 67−76.
(36) Kichler, A. Gene Transfer with Modified Polyethylenimines. *J. Gene Med.* **2004**, *6*, S3−S10.
(37) Hofmann, A.; Thierbach, S.; Semisch, A.; Hartwig, A.; Taupitz, M.; Ruhl, E.; Graf, C. Highly Monodisperse Water-Dispersable Iron Oxide Nanoparticles for Biomedical Applications. *J. Mater. Chem.* **2010**, *20*, 7842−7853.
(38) Hondow, N.; Brydson, R.; Wang, P.; Holton, M.; Brown, M. R.; Rees, P.; Summers, H.; Brown, A. Quantitative Characterization of Nanoparticle Agglomeration within Biological Media. *J. Nanopart. Res.* **2012**, *14*, 977.
(39) Filipe, V.; Hawe, A.; Jiskoot, W. Critical Evaluation of Nanoparticle Tracking Analysis (NTA) by NanoSight for the Measurement of Nanoparticles and Protein Aggregates. *Pharm. Res.* **2010**, *27*, 796−810.
(40) Park, K.; Kim, J.; Nam, Y. S.; Lee, S.; Nam, H. Y.; Kim, K.; Park, J. H.; Kim, I.; Choi, K.; Kim, S. Y.; Kwon, I. C. Effect of Polymer Molecular Weight on the Tumor Targeting Characteristics of Self-Assembled Glycol Chitosan Nanoparticles. *J. Controlled Release* **2007**, *122*, 305−314.
(41) Lungwitz, U.; Breunig, M.; Liebl, R.; Blunk, T.; Goepferich, A. Methoxy Poly(Ethylene Glycol)-Low Molecular Weight Linear Polyethylenimine-Derived Copolymers Enable Polyplex Shielding. *Eur. J. Pharm. Biopharm.* **2008**, *69*, 134−148.
(42) Germershaus, O.; Mao, S.; Sitterberg, J.; Bakowsky, U.; Kissel, T. Gene Delivery Using Chitosan, Trimethyl Chitosan or Polyethylenglycol-Graft-Trimethyl Chitosan Block Copolymers: Establishment of Structure-Activity Relationships in Vitro. *J. Controlled Release* **2008**, *125*, 145−154.
(43) He, C. B.; Hu, Y. P.; Yin, L. C.; Tang, C.; Yin, C. H. Effects of Particle Size and Surface Charge on Cellular Uptake and Biodistribution of Polymeric Nanoparticles. *Biomaterials* **2010**, *31*, 3657−3666.
(44) Mohan, P.; Rapoport, N. Doxorubicin as a Molecular Nanotheranostic Agent: Effect of Doxorubicin Encapsulation in Micelles or Nanoemulsions on the Ultrasound-Mediated Intracellular Delivery and Nuclear Trafficking. *Mol. Pharmaceutics* **2010**, *7*, 1959−1973.

DOI: 10.1021/acsami.5b05335
ACS Appl. Mater. Interfaces 2015, 7, 21254−21262